conditions 6 ($k_{2Z} \gg k_{3Z}$) and 7 ($k_{3A} \gg k_{-1A}$) of the text are introduced.

There are two ways of examining eq 6. First, since $k_{3A} \gg k_{-1A}$, eq 6 requires that k_{-3A}[Ac-Phe] >>> k_{-3Z}[Z-Ala-His-Phe]. Given that [Ac-Phe] = 25 mM and [Z-Ala-His-Phe] = 1 mM, it appears that the rate constant for reaction of E-Trp with Ac-Phe, k_{-3A}, exceeds k_{-3Z}, that for reaction between E-Trp and Z-Ala-His-Phe. An alternative treatment of eq 6 makes the reasonable assumption that the equilibrium constants for hydrolysis of Ac-Phe-Trp and Z-Ala-His-Phe-Trp via the amino-enzyme route (lower path of eq 2) are identical, so that $(k_{1A}k_{3A}/K_Ak_{-1A}k_{-3A}) = (k_{1Z}k_{3Z}/K_Zk_{-1Z}k_{-3Z})$. Since the relative rates of hydrolysis of the two peptides suggest that $(k_{1Z}/K_Z) \simeq 100(k_{1A}/K_A)$ (Table I, ref 13, and eq 2), $(k_{3A}/k_{-3Z}/k_{-1A}k_{-3A}) \simeq 100(k_{3Z}/k_{-1Z})$. Equation 6 reduces to eq 7 when the values for [Z-Ala-His-Phe] and [Ac-Phe] are introduced.

$$0.75k_{-1Z} >> k_{3Z} \quad (7)$$

References and Notes

(1) M. S. Silver and M. Stoddard, *Biochemistry*, **11**, 191 (1972).
(2) For reviews, see (a) J. R. Knowles, *Phil. Trans. R. Soc., London, Ser. B*, **257**, 135 (1970); (b) G. E. Clement, *Prog. Bioorg. Chem.*, **2**, 177 (1973); (c) J. S. Fruton, *Acc. Chem. Res.*, **7**, 241 (1974).
(3) M. Takahashi and T. Hofmann, *Biochem. J.*, **147**, 549 (1975), and earlier papers by Hofmann and co-workers.
(4) A. K. Newmark and J. R. Knowles, *J. Am. Chem. Soc.*, **97**, 3557 (1975).
(5) G. P. Sachdev and J. S. Fruton, *Proc. Natl. Acad. Sci. U.S.A.*, **72**, 3424 (1975).
(6) (a) H. Neumann, Y. Levin, A. Berger, and E. Katchalski, *Biochem. J.*, **73**, 33 (1959); (b) J. S. Fruton, S. Fujii, and M. H. Knappenberger, *Proc. Natl. Acad. Sci. U.S.A.*, **47**, 759 (1961).
(7) All amino acids possess the L configuration except where specifically noted otherwise.
(8) Acceptors are generally acylated L-amino acid derivatives.
(9) The experiment is conceptually related to that of N. I. Mal'tsev, L. M. Ginodman, V. N. Orekhovich, T. A. Valueva, and L. N. Akimova, *Biokhimiya*, **31**, 983 (1966).
(10) T. M. Kitson and J. R. Knowles, *Biochem. J.*, **122**, 249 (1971).
(11) E. Stahl, "Thin-Layer Chromatography", 2d ed, Springer-Verlag, New York, N.Y., 1969.
(12) J. L. Denburg, R. Nelson, and M. S. Silver, *J. Am. Chem. Soc.*, **90**, 479 (1968).
(13) M. S. Silver and M. Stoddard, *Biochemistry*, **14**, 614 (1975).
(14) K. Inouye, I. M. Voynick, G. R. Delpierre, and J. S. Fruton, *Biochemistry*, **5**, 2473 (1966).
(15) G. A. Bray, *Anal. Biochem.*, **1**, 279 (1960).
(16) (a) L. M. Ginodman, N. G. Lutsenko, T. N. Barshevskaya, and V. V. Somova, *Biokhimiya*, **36**, 604 (1971); (b) T. A. Valueva, L. M. Ginodman, T. N. Barshevskaya, and F. T. Guseinov, *ibid.*, **38**, 435 (1973).
(17) L. M. Ginodman and N. G. Lutsenko, *Biokhimiya*, **37**, 101 (1972).
(18) V. K. Antonov, L. O. Rumsh, and A. G. Tikhodeeva, *Bioorg. Khim.*, **1**, 993 (1975).
(19) Unpublished experiments in this laboratory.

On the Correlation between Three-Dimensional Structure and Reactivity for a Series of Locked Substrates of Chymotrypsin

P. S. Rodgers,*[1a] L. C. G. Goaman,[1a] and D. M. Blow[1b]

Contributions from the Department of Physics, Portsmouth Polytechnic, Portsmouth, England, and MRC Laboratory of Molecular Biology, Cambridge, England.

Received June 7, 1975

Abstract: The crystal structure of D-methyl 1,2-dihydronaphtho[2,1-*b*]furan-2-carboxylate (D-I), a "locked" substrate of chymotrypsin, has been determined using Patterson search methods and refined to an *R* factor of 0.10. The molecule adopted a pseudoaxial conformation in the crystal lattice. The dihydrofuran ring was buckled 18° with respect to the plane of the aromatic part of the molecule and the ring was found to be highly strained and asymmetric. Using the bond lengths found crystallographically, it has been possible to make reasonable predictions about the geometry of the molecule in the equatorial form (which is the probable conformation adopted by the molecule in the enzyme active site) and to establish the precise differences in shape between the isomers of I and those of methyl 2,3-dihydronaphtho[1,2-*b*]furan-2-carboxylate (II) and methyl 4,5-benzindan-2-carboxylate (III). With the aid of accurate model fitting studies on the active site of chymotrypsin, these differences in geometry have been correlated with the widely divergent kinetic behavior of these molecules toward the enzyme.

Systematic studies of the kinetics of hydrolyses catalyzed by chymotrypsin have yielded a wealth of information on the structural features required of a good substrate by the enzyme and on their likely role in the catalytic process.[2,3]

A large range of cyclized substrates with restricted conformational freedom has been investigated in order to obtain a more precise estimate of the spatial arrangement of the functional groups in the substrate when bound productively in the enzyme active site.[4-8] Of all the "locked" substrates so far prepared, D-methyl 1,2-dihydronaphtho[2,1-*b*]furan-2-carboxylate (D-I) has the highest D/L stereospecificity,[4] 34 000. The ester group of D-I can adopt either a pseudoaxial or a pseudoequatorial conformation with respect to the planar aromatic part of the molecule. Lawson[4] has maintained that only in the axial form would D-I and L-I be sufficiently different in overall shape to account adequately for the observed large difference in their reactivity toward chymotrypsin. Cohen[7a] and Silver,[6] however, came to the opposite conclusion from similar kinetic studies on other locked substrates and favor the equatorial form as the productive binding mode.

The crystallographic work of Steitz et al.[9] on the enzyme itself clearly shows that the ester group of the substrate must lie near the plane of the aromatic side chain in order to be attacked by O^{γ}-(Ser-195) so that D-I would bind productively in the equatorial mode. Blow[10] has suggested that the D/L specificity of I arises from more subtle differences in orientation of the ester group between D-I and L-I, emphasizing the exactness of fit which a good locked substrate must achieve.

The aim of this present work has therefore been to obtain reliable bond length and angle information from the crystal structure of D-I in order to determine just how different D-I and L-I would actually be in the equatorial conformation.

Table I. Kinetic Constants for Substrates I–IV

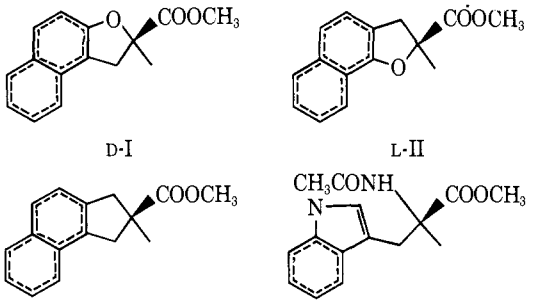

	K_m, mM	$k_{cat.}$, s^{-1}	k_{OH}, s^{-1} [a]	$[k_{cat.}/K_m]_{H_2O}$ [b]
D-I	1.46	5.88	50.0	1.7×10^4
L-I	25.0	0.0027		0.5
D-II	77.0	5.68	35.0	44.0
L-II	14.9	0.28		12.0
(+)-III	28.6	0.0028	0.42	4.8
(−)-III	1.94	0.039		1.0×10^3
D-IV			0.57	0.17
L-IV	7.4	49.5		1.85×10^5

[a] k_{OH} is the intrinsic rate of nonenzymic hydrolysis by hydroxide ions. [b] $[k_{cat.}/K_m]_{H_2O}$ is the extrapolated value of the normalized activity constant $[k_{cat.}/(K_m \cdot k_{OH})]$ for aqueous solutions.[4,5]

Similar deductions may then also be made about the closely related compounds, methyl 2,3-dihydronaphtho[1,2-*b*]-furan-2-carboxylate (II) and methyl 4,5-benzindan-2-carboxylate (III), for which the kinetic constants are given in Table I. The correlation between overall geometry and reactivity toward chymotrypsin among the isomers of compounds I, II, and III gives useful information about the closeness of fit required of a good substrate by the enzyme.

Experimental Section

Transparent needle-shaped crystals were grown from a solution of D-I in methanol at −5 °C. The space group was found to be $P2_12_12_1$ with four molecules in the unit cell. Accurate unit cell dimensions were obtained from zero-level Weissenberg photographs calibrated by the superposition of a Weissenberg powder pattern from a gold wire. The results obtained were $a = 5.020 \pm 0.007$ Å, $b = 11.519 \pm 0.009$ Å, and $c = 19.626 \pm 0.009$ Å. Five levels of data (up to $h = 4$) were collected with the crystal mounted about the needle axis by the multifilm equi-inclination Weissenberg photographic method using nickel-filtered Cu Kα radiation and five films to each pack. Intensities were measured by visual comparison with a calibrated wedge. 1160 unique nonzero reflections out of the total of 1297 possible reflections were obtained and Lorentz, polarization, and spot-shape corrections were applied. Interlayer scales, absolute scales, and mean isotropic temperature factors were calculated from Wilson plots.[11]

The structure of D-I was solved using the three-step Patterson-search procedure described by Tollin et al.[12-14] The method is applicable to molecules possessing a substantially planar structure and consists of locating from the Patterson map, firstly, the plane of maximum electron density; secondly, the orientation of the planar molecular fragment in this plane; and, thirdly, calculating the displacement of the oriented planar fragment from the symmetry elements present in the cell.

A sharpened Patterson map was calculated using the Wunderlich sharpening function[16] $M(s) = (1/\hat{f}_j^2) \cosh(as) \exp(-\pi^2 s^2/p)$ with constants $a = 8.0$, $p = 0.7$. The plane of maximum density in this map was calculated using the $I(\theta,\phi)$ function defined by Tollin and Cochran.[12] To reduce computation time only the 400 most intense reflections were used. The total density on the surface of a disk of radius 3.5 Å centered on the Patterson origin was calculated at 2° increments on the spherical polar angles θ, ϕ over the unique octant of Patterson space $\theta = 0 \rightarrow 90°$, $\phi = 0 \rightarrow 90°$. The results are shown plotted as a Sanson-Flamsteed equal area projection in Figure 1 and clearly indicate that the normal to the plane of maximum density has coordinates $\theta = 68°$, $\phi = 39°$.

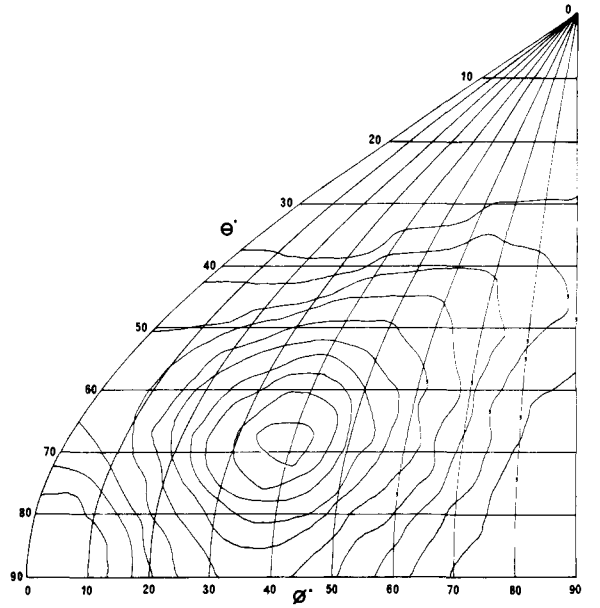

Figure 1. Sanson-Flamsteed equal area projection of the $I(\theta,\phi)$ function for D-I. The plane of maximum density has $\theta = 68°$ and $\phi = 39°$. Contours are at 10^4 e^2 intervals.

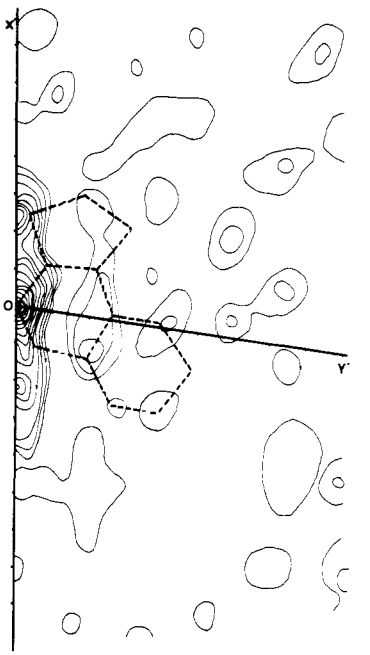

Figure 2. Patterson section at $\theta = 68°$, $\theta = 39°$, showing orientation of the planar fragment of D-I. OX' is the intersection of the $I(\theta,\phi)$ plane and the plane $Y = 0$. OY' is perpendicular to OX' in the plane. The scale of the map is 1 division = 1 Å. The map is scaled to give an origin peak height of 10^3 e^2.

The program DPATS[15] was used to calculate a Patterson section in this plane. By superposing a transparent, suitably scaled vector set of the planar naphthofuran ring system of D-I on this map, the orientation of the planar part of the molecule was obtained (Figure 2). With atom C_3 arbitrarily placed at the origin, the relative coordinates of the remaining atoms in the planar fragment were calculated.

The real space displacement of the oriented planar fragment from the screw axes was obtained using the Q function defined by Tollin.[14] The maps so produced (Figure 3) are sum functions of the projection Patterson map perpendicular to a screw axis (calculated from the observed reflection intensities) and the Patterson map based on the chosen displacement of the oriented fragment from the symmetry element. Since in space group $P2_12_12_1$ it is conventional to choose the origin such that the screw axes pass through (0¼0, 00¼, ¼00), a displacement of a ¼ of a cell in the appropriate direction was incor-

Table II. Fractional Coordinates and Anisotropic Thermal Parameters for Heavy Atoms[a]

	x	y	z	b_{11}	b_{12}	b_{13}	b_{22}	b_{23}	b_{33}
C(1)	0.748 (2)	0.5088 (5)	0.0442 (3)	473	−19	−8	84	−22	31
C(2)	0.885 (1)	0.4131 (5)	0.0641 (3)	454	−8	−8	85	−5	35
C(3)	1.068 (2)	0.3546 (6)	0.0227 (3)	622	55	5	103	−27	41
C(4)	1.110 (2)	0.4004 (6)	−0.0411 (3)	498	−21	14	117	−40	47
C(5)	1.015 (2)	0.5454 (7)	−0.1308 (3)	545	−40	7	141	−17	39
C(6)	0.875 (2)	0.6381 (8)	−0.1531 (3)	769	−302	25	176	−14	32
C(7)	0.680 (2)	0.6927 (6)	−0.1110 (3)	699	−43	−93	121	5	42
C(8)	0.631 (2)	0.6512 (5)	−0.0458 (3)	563	−28	−28	105	−6	33
C(9)	0.783 (1)	0.5556 (5)	−0.0215 (3)	455	−54	−16	92	−15	32
C(10)	0.971 (1)	0.5010 (6)	−0.0648 (3)	483	−54	12	110	−28	35
C(11)	0.562 (2)	0.5479 (6)	0.1013 (3)	431	45	27	124	−4	30
C(12)	0.666 (1)	0.4685 (5)	0.1598 (3)	465	−38	−8	92	−3	34
C(13)	0.850 (2)	0.5314 (5)	0.2103 (3)	709	−98	42	103	−12	25
C(14)	0.854 (2)	0.6897 (7)	0.2888 (4)	991	−77	−118	138	−21	45
O(1)	0.817 (1)	0.3757 (3)	0.1293 (3)	747	44	−3	92	−8	35
O(2)	1.072 (1)	0.5085 (5)	0.2219 (3)	305	98	−33	225	−51	51
O(3)	0.712 (1)	0.6201 (4)	0.2375 (3)	710	57	−73	109	−29	39

[a] The thermal parameters, $b_{ij} \times 10^4$, are the coefficients in the expression, $B_{\text{aniso}} = \exp[-(b_{11}h^2 + b_{12}hk + b_{13}hl + b_{22}k^2 + b_{23}kl + b_{33}l^2)]$. Estimated deviations in the last digit in the fractional coordinates are given in parentheses.

Table III. Fractional Coordinates of Hydrogen Atoms and Isotropic Thermal Parameters

	x	y	z	B_{iso}, Å^2
H(1)	0.36 (1)	0.542 (5)	0.093 (3)	3.0
H(2)	0.57 (1)	0.639 (5)	0.115 (3)	2.9
H(3)	1.13 (2)	0.278 (6)	0.043 (3)	5.2
H(4)	1.24 (2)	0.348 (7)	−0.078 (4)	9.2
H(5)	1.20 (2)	0.497 (6)	−0.162 (3)	6.2
H(6)	0.88 (1)	0.683 (5)	−0.195 (3)	4.2
H(7)	0.62 (2)	0.769 (6)	−0.124 (3)	6.4
H(8)	0.56 (1)	0.704 (5)	−0.020 (3)	3.5
H(9)	0.88 (2)	0.774 (6)	0.270 (4)	7.0
H(10)	1.02 (2)	0.692 (6)	0.281 (4)	7.7
H(11)	0.94 (2)	0.625 (6)	0.325 (3)	5.3
H(12)	0.47 (2)	0.432 (6)	0.186 (4)	7.4

porated into the program so that the origin of the maps in Figure 3 corresponds to the unit cell origin rather than to the screw axes. The peak marked A on each of these maps shows that the displacement of C_3 from the unit cell origin was 0.058, 0.355, 0.030. By adding this displacement to the relative coordinates of the remaining atoms of the planar fragment, as derived by DPATS, the real space coordinates of these atoms were obtained.

After least-squares refinement of these coordinates, the residual R factor was 0.30 which was taken as indicative that the correct orientation of the fragment had been chosen. The electron density map calculated on the basis of these coordinates showed additional peaks where the ester group would be expected and after inserting these atoms into the calculations the least-squares refinement proceeded smoothly to 0.20. At this stage hydrogen atoms became visible on the difference electron density map. The nonhydrogen atoms were refined anisotropically and the final R factor reached was 0.10. The weighting scheme used was

$$\omega = [1 + (F_{\text{obsd}} - F^*)^2/G^*]^{-1}$$

where $F^* = 10.0$, $G^* = 20.0$. Fractional coordinates and thermal parameters for nonhydrogen atoms are listed in Table II and for hydrogen atoms in Table III.

Results

Figure 4 shows the [010] projection of D-I and the atom-labeling scheme used. Bond lengths and angles are listed in Tables IV and VI.

The first point to note from Figure 4 is that D-I crystallizes in the axial conformation which therefore represents the lowest energy conformation in the crystals, where some stabilization may be due to intermolecular forces in the crystal lattice. Table V shows the distances of atoms from the best fit plane through the naphthalene rings. C_{12} is 0.26 Å out of the plane and the

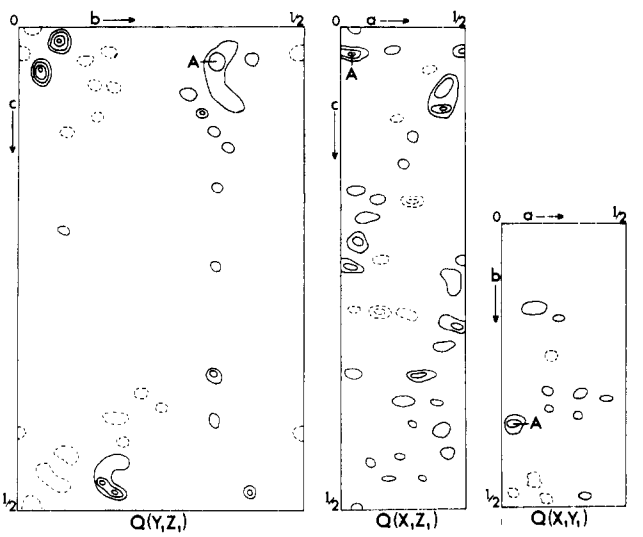

Figure 3. The Q-function maps for D-I. The position of the peak A gives the displacement of the Patterson origin (in Figure 2) from the unit cell origin.

ester group carbon atom, C_{13}, is 1.72 Å from the plane on the same side of the plane as C_{12} so that the C_{12}–C_{13} bond is almost perpendicular to the aromatic plane.

The furan ring is significantly buckled. The angle between the aromatic plane and the plane through atoms C_{11}, C_{12}, and O_1 is 18.4° which agrees well with the value of 19° reported by Green[17] for the related 2,3-dihydrofuran molecule from infrared measurements.

Table VI indicates that the furan ring in D-I is highly strained; in particular, the angle C_1–C_{11}–C_{12} of 99.3° is unusually small. The fact that the C_2–O_1 (1.39 Å) and O_1–C_{12} (1.44 Å) bonds are considerably shorter than C_1–C_{11} (1.53 Å) and C_{11}–C_{12} (1.56 Å) results in the furan ring being highly asymmetric when viewed perpendicularly to the aromatic plane. C_{12} is displaced 0.18 Å to the O_1 side of the meridian line through the midpoints of the C_1–C_2 and C_4–C_{10} bonds (see Figure 4) and C_{13} is 0.21 Å to the same side of the meridian line.

On the assumption that the furan ring would be equally buckled in the axial and equatorial forms, the positions of atoms C_{12} and C_{13} in the latter form were calculated by rotating the C_{12}–C_{13} bond by 36.8° about an axis through C_{11}–O_1. It was then found that the displacement of C_{13} from the meridian line in projection perpendicular to the aromatic

Table IV. Bond Lengths (Å) with Esd's

H_1-C_{11}	1.04 (7)	C_2-C_3	1.402 (11)
H_2-C_{11}	1.09 (6)	C_2-O_1	1.394 (8)
H_3-C_3	1.04 (7)	C_3-C_4	1.372 (10)
H_4-C_4	1.16 (9)	C_4-C_{10}	1.430 (10)
H_5-C_5	1.24 (8)	C_5-C_6	1.351 (12)
H_6-C_6	0.98 (6)	C_5-C_{10}	1.411 (10)
H_7-C_7	0.97 (8)	C_6-C_7	1.427 (12)
H_8-C_8	0.88 (6)	C_7-C_8	1.389 (10)
H_9-C_{14}	1.05 (7)	C_8-C_9	1.422 (10)
$H_{10}-C_{14}$	0.87 (9)	C_9-C_{10}	1.420 (10)
$H_{11}-C_{14}$	1.12 (7)	$C_{11}-C_{12}$	1.558 (9)
$H_{12}-C_{12}$	1.16 (9)	$C_{12}-C_{13}$	1.535 (10)
C_1-C_2	1.356 (9)	$C_{12}-O_1$	1.442 (8)
C_1-C_9	1.409 (8)	$C_{13}-O_2$	1.171 (10)
C_1-C_{11}	1.527 (9)	$C_{13}-O_3$	1.346 (9)
		$C_{14}-O_3$	1.473 (10)

Table V. Deviations (Å) from Planarity of Atoms in Molecule[a]

C(1)	−0.032	C(8)	0.031
C(2)	−0.001	C(9)	−0.022
C(3)	0.034	C(10)	−0.019
C(4)	0.014	C(11)	−0.033
C(5)	−0.021	C(12)	−0.270
C(6)	−0.005	C(13)	−1.717
C(7)	0.027	O(1)	0.043

[a] Distances from least-squares best fit plane through atoms C_1-C_{10}. This plane has direction cosines −0.7155, −0.6009, −0.3564 and coefficients −0.1103, −0.0927, −0.0550.

Table VI. Bond Angles (Deg) with Esd's

$H_1-C_{11}-H_2$	98 (5)	$C_1-C_2-C_3$	124.0 (6)
$H_1-C_{11}-C_1$	118 (3)	$C_1-C_2-O_1$	113.1 (6)
$H_1-C_{11}-C_{12}$	115 (3)	$C_1-C_9-C_8$	122.5 (6)
$H_2-C_{11}-C_1$	117 (3)	$C_1-C_9-C_{10}$	117.5 (6)
$H_2-C_{11}-C_{12}$	112 (3)	$C_1-C_{11}-C_{12}$	99.3 (5)
$H_3-C_3-C_2$	113 (4)	$C_2-C_1-C_9$	120.7 (6)
$H_3-C_3-C_4$	130 (4)	$C_2-C_1-C_{11}$	109.9 (5)
$H_4-C_4-C_3$	118 (4)	$C_2-C_3-C_4$	116.2 (7)
$H_4-C_4-C_{10}$	119 (4)	$C_2-O_1-C_{12}$	106.2 (5)
$H_5-C_5-C_6$	126 (3)	$C_3-C_2-O_1$	122.9 (6)
$H_5-C_5-C_{10}$	114 (3)	$C_3-C_4-C_{10}$	122.4 (7)
$H_6-C_6-C_5$	133 (4)	$C_4-C_{10}-C_5$	121.2 (7)
$H_6-C_6-C_7$	106 (4)	$C_4-C_{10}-C_9$	119.2 (6)
$H_7-C_7-C_6$	119 (4)	$C_5-C_6-C_7$	121.2 (7)
$H_7-C_7-C_8$	119 (4)	$C_5-C_{10}-C_9$	119.6 (6)
$H_8-C_8-C_7$	112 (4)	$C_6-C_5-C_{10}$	120.2 (7)
$H_8-C_8-C_9$	125 (4)	$C_6-C_7-C_8$	120.2 (7)
$H_9-C_{14}-H_{10}$	79 (7)	$C_7-C_8-C_9$	118.8 (7)
$H_9-C_{14}-H_{11}$	144 (6)	$C_8-C_9-C_{10}$	120.0 (6)
$H_9-C_{14}-O_3$	108 (4)	$C_9-C_1-C_{11}$	129.4 (6)
$H_{10}-C_{14}-H_{11}$	75 (6)	$C_{11}-C_{12}-C_{13}$	113.7 (5)
$H_{10}-C_{14}-O_3$	112 (5)	$C_{11}-C_{12}-O_1$	107.9 (5)
$H_{11}-C_{14}-O_3$	105 (4)	$C_{12}-C_{13}-O_2$	126.3 (6)
$H_{12}-C_{12}-C_{11}$	105 (4)	$C_{12}-C_{13}-O_3$	107.8 (6)
$H_{12}-C_{12}-C_{13}$	113 (4)	$C_{13}-C_{12}-O_1$	107.6 (6)
$H_{12}-C_{12}-O_1$	110 (4)	$C_{13}-O_3-C_{14}$	115.7 (6)
		$O_2-C_{13}-O_3$	125.8 (7)

plane increased to 0.26 Å and that the displacement perpendicular to the plane was now 0.58 Å (see Figure 5).

In view of the apparent conflict between the predictions of an equatorial binding mode to the enzyme and the finding of an axial form of D-I in the crystals, a series of NMR studies (to be reported fully elsewhere) was undertaken to determine the magnitude of the energy difference between the two conformations. The results showed that, as expected, the axial form had the lower energy, but that the energy difference between the two forms was very small, ranging from nearly 1 kJ/mol in the more polar solvent, methanol, to near zero in the less polar solvent, chloroform. Since the active site of chymotrypsin was known to be hydrophobic,[18] it was assumed that the energy difference between the conformers of D-I was

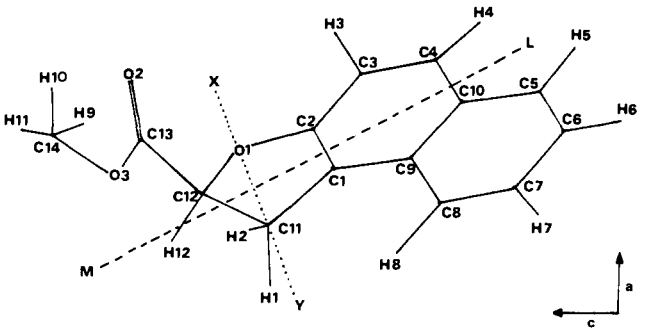

Figure 4. [010] projection of D-I showing the atom-labeling scheme. The meridian line ML passes through the midpoints of the C_1-C_2 and C_4-C_{10} bonds. The line *XY* is the axis about which the furan ring buckles to give either an axial or an equatorial conformation for the ester group.

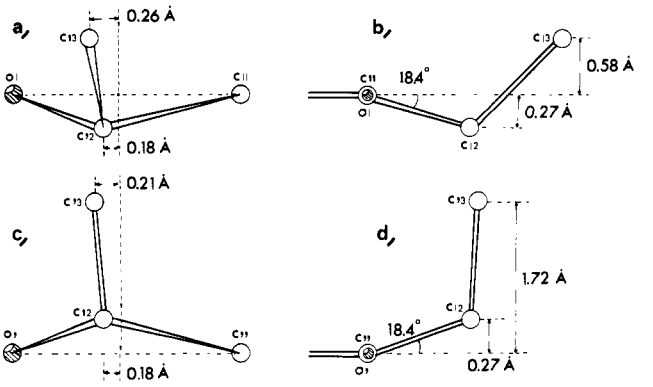

Figure 5. (a) D-I equatorial form viewed down the meridian line (ML in Figure 4). (b) D-I equatorial form viewed down the axis through C_{11} and O_1 (*XY* in Figure 4). (c) and (d) are the corresponding views of the axial form of D-I.

negligibly small and that the postulation of an equatorial binding mode did not imply that the substrate was binding in a significantly high-energy conformation.

At this stage an accurate model of the active site of chymotrypsin was constructed from the refined coordinates of the enzyme published by Birktoft and Blow.[19] Attempts were then made to fit scale models of D/L-I, D/L-II, (±)-III into the active site in both axial and equatorial conformations. It was assumed that in the productive binding mode the aromatic part of the substrate must reside centrally in the active site cleft, the ester group carbon atom must be within reacting distance of serine-195 [probably about 3.0 Å from C^{β}-(Ser-195)], and that the plane of the ester group is approximately at right angles to the direction of attack by O^{γ}-(Ser-195) as proposed by Henderson.[20] Table VII lists the coordinates of D-I in the enzyme active site along with the closest enzyme–substrate contacts. The carbonyl oxygen atom forms hydrogen bonds with NH-(Gly-193) and NH-(Ser-195), thus holding the ester group at the correct angle for nucleophilic attack by O^{γ}-(Ser-195). Figure 6 gratifyingly shows that the proposed orientation of D-I in the active site is, in fact, very similar to that found by Steitz et al.[9] for its open-chain counterpart *N*-formyl-L-tryptophan bound to the crystalline enzyme. It is noteworthy that the axial form of D-I could not be fitted satisfactorily into the active site, thus further confirming that the equatorial mode is the productive one.

Discussion

The x-ray work on D-I reported above has shown that in the equatorial form, the ester group carbon atom, C_{13}, is 0.58 Å from the aromatic plane. It is reasonable to suppose, therefore, that in the opposite enantiomer, L-I, this atom would be a similar distance on the opposite side of the aromatic plane. A

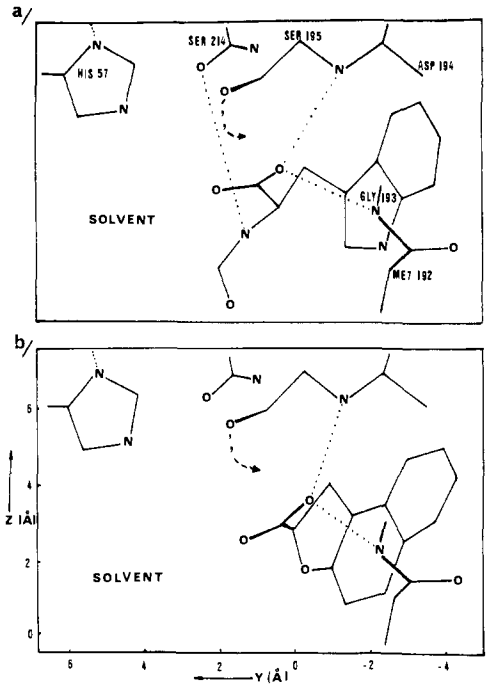

Figure 6. [100] projections of (a) *N*-formyltryptophan[9] and (b) D-I in the active site of chymotrypsin showing enzyme–substrate hydrogen bonds. The coordinate system is as defined by Birktoft et al.[23]

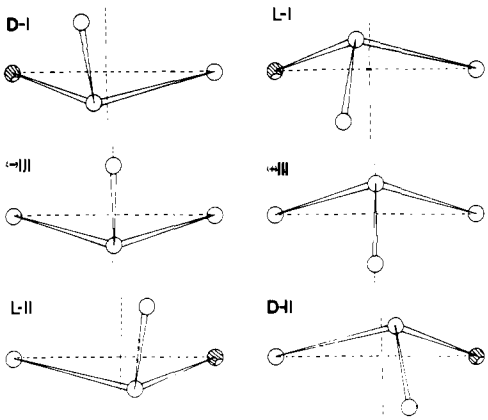

Figure 7. A comparison of the geometry of the isomers of compounds I–III in their equatorial form viewed down the meridian line (ML in Figure 4). It is the ester carbon atom C_{13} which undergoes nucleophilic attack by O^{γ}-(Ser-195) in the catalytic reaction.

difference in position of 1.16 Å for the electrophilic carbon, C_{13}, between D-I and L-I is more than sufficient to account for the vastly different rates of hydrolysis of these compounds by chymotrypsin. This sizable difference between the two equatorial isomers of I therefore removes Lawson's principal objection to the equatorial binding hypothesis. Further consideration of the possible binding of L-I to the active site shows that for this isomer axial binding is distinctly possible with the naphthofuran ring occupying the same position in the active site as for D-I but with the ester group in the vicinity of Ser-214 and partially exposed to solvent. This nonproductive binding would still further reduce the reactivity of L-I relative to D-I. It may well be that it is the extreme *un*reactivity of L-I rather than the modest reactivity of D-I which accounts for the observed high D/L stereospecificity of I. This in turn points to a general limitation to the use of stereospecificity ratios as a criterion for deciding whether a particular substance is a good substrate or not.[6,21]

If it is assumed that the furan rings in I and II have similar

Table VII. Active Site Coordinates (Å) of D-I

	x	*y*	*z*
C(1)	18.01	−1.40	4.86
C(2)	17.92	−0.95	3.56
C(3)	18.78	−1.36	2.53
C(4)	19.79	−2.25	2.89
C(5)	20.92	−3.69	4.56
C(6)	21.00	−4.20	5.84
C(7)	20.07	−3.81	6.82
C(8)	19.07	−2.90	6.52
C(9)	18.99	−2.34	5.22
C(10)	19.91	−2.76	4.23
C(11)	16.91	−0.77	5.71
C(12)	16.41	+0.29	4.69
C(13)	14.88	+0.50	4.73
C(14)	12.84	1.62	4.38
O(1)	16.89	−0.07	3.40
O(2)	14.28	−0.38	5.15
O(3)	14.28	1.54	4.14

Shortest D-I to Enzyme Distances (Å)	
C_4–$O^{\prime}$-(Ser-217)	3.33[a]
C_5–*N*-(Ser-217)	3.44[a]
C_7–C^{β}-(Ser-190)	3.35[a]
C_{13}–O^{γ}-(Ser-195)	2.99[b]
O_2–C^{β}-(Ser-195)	2.90[b]
O_2–O^{γ}-(Ser-195)	3.08[b]
O_2–C^{β}-(Met-192)	3.39[b]
O_2–*N*-(Gly-193)	3.06[c]
O_2–*N*-(Ser-195)	2.95[c]

[a] Hydrophobic binding interactions in active site cleft. [b] Short van der Waals contact distances relieved by formation of tetrahedral intermediate. [c] Hydrogen bonds holding carboxylate group in correct orientation for catalytic attack by O^{γ}-(Ser-195).

bond lengths and angles and that the five-membered ring in III is symmetrical, further correlations may be made between structure and reactivity among these compounds. Figure 7 shows the geometrical relationships between D/L-I, D/L-II, and (±)-III in their equatorial form and Table I shows the kinetic constants for their enzymic hydrolysis. D-I and L-II are related by a local mirroring of the ester group and furan ring across a plane through the meridian line M (viewed end on in Figure 7) and at right angles to the aromatic plane. C_{13} differs in position by 0.52 Å from D-I to L-II in the equatorial form and results in a 15-fold drop in $k_{cat.}$ and a tenfold increase in K_m. The latter increase has been satisfactorily explained by Lawson[5] as arising from the adverse effect of burying the furan oxygen in the hydrophobic interior of the active site. If the naphthalene ring system in L-II occupied precisely the same position in the active site as for D-I, C_{13} would be 0.52 Å closer to C^{β}-(Ser-195) than for the latter. Since, however, this contact is already short (3.0 Å) even for D-I, one is forced to conclude that, rather than make this contact even shorter, the molecule of L-II must rotate in the binding cleft a corresponding distance away from the active serine. This results in a slightly incorrect orientation of the ester group for optimum catalytic hydrolysis to take place and readily accounts for the 15-fold lower value of $k_{cat.}$ relative to D-I.

By contrast, L-I and D-II only differ by a factor of 3 in K_m but $k_{cat.}$ for L-I is more than 2×10^3 times lower than for D-II (see Table I) even though in the equatorial mode they, too, would differ in the position of C_{13} by 0.52 Å. A nonproductive axial binding mode has already been suggested for L-I but model building studies suggest that such a conformation is not accessible to D-II due to interference with CO-(Ser-214). This contrast illustrates the unsymmetrical nature of the potential energy profile for the binding of substrates to the active site. A 0.5-Å movement in one direction may cause very different kinetic effects from a similar movement in another direction.

For comparisons between D/L-I and (±)-III to be meaningful, account must be taken of the fact that the intrinsic reactivity of the latter toward nonenzymic alkaline hydrolysis is almost 200 times lower than for the former.[5] After allowing for this, D-I and (−)-III have almost identical rates of catalysis by the enzyme which therefore appears to be able to accommodate the 0.26-Å difference in position of C_{13} without loss of activity. When the opposite isomers, L-I and (+)-III, are compared, it is again evident that L-I is an exceedingly poor substrate and that its axial form may perhaps be the predominant binding conformation.

Conclusion

While a limited survey such as this cannot hope to provide sufficient data to map the general relationships between structure and reactivity of substrates, the tentative conclusion may be drawn that, for this particular series of compounds, differences in the geometry of the functional groups of the order of 0.25 Å may be accommodated by the enzyme without significant loss of catalytic activity while differences of 0.5 Å may cause changes in reactivity ranging from 15- to 2000-fold depending on the nature and direction of such a displacement. This, therefore, gives a semiquantitative estimate of the closeness of fit required of these substrates by the active site of chymotrypsin.

Acknowledgments. We thank Dr. W. B. Lawson for kindly supplying the samples of substrates used in this work and Messrs. Cross, Griffiths, and Powell for the use of their computer programs.[22] P. S. Rodgers thanks the Governors of Portsmouth Polytechnic for a postgraduate Research Assistantship to finance this work.

Supplementary Material Available: Listings of structure factors (8 pages). Ordering information is given on any current masthead page.

References and Notes

(1) (a) Portsmouth Polytechnic; (b) MRC Laboratory of Molecular Biology.
(2) (a) G. E. Hein and C. Niemann, *Proc. Natl. Acad. Sci. U.S.A.*, **47**, 1341 (1961); (b) B. Zerner and M. L. Bender, *J. Am. Chem. Soc.*, **86**, 3669 (1964).
(3) D. W. Ingles and J. R. Knowles, *Biochem. J.*, **108**, 561 (1968).
(4) Y. Hayashi and W. B. Lawson, *J. Biol. Chem.*, **244**, 4158 (1969).
(5) T. N. Pattabiraman and W. B. Lawson, *J. Biol. Chem.*, **247**, 3029 (1972).
(6) M. S. Silver, M. Stoddard, T. Sone, and M. S. Matta, *J. Am. Chem. Soc.*, **92**, 3151 (1970).
(7) (a) S. G. Cohen and R. M. Schultz, *J. Biol. Chem.*, **243**, 2607 (1968); (b) S. G. Cohen, A. Milovanovic, R. M. Schultz, and S. Y. Weinstein, *ibid.*, **244**, 2664 (1969).
(8) L. D. Rumsh, L. I. Volkova, and V. K. Antonov, *FEBS Lett.*, **9**, 64 (1970).
(9) T. A. Steitz, R. Henderson, and D. M. Blow, *J. Mol. Biol.*, **46**, 337 (1969).
(10) D. M. Blow in "The Enzymes", Vol. III, P. D. Boyer, Ed., Academic Press, New York, N.Y., 1971, pp 185–212.
(11) A. J. C. Wilson, *Nature (London)*, **150**, 152 (1942).
(12) P. Tollin and W. Cochran, *Acta Crystallogr.*, **17**, 1322 (1964).
(13) P. Tollin, P. Main, and M. G. Rossmann, *Acta Crystallogr.*, **20**, 404 (1966).
(14) P. Tollin, *Acta Crystallogr.*, **21**, 613 (1966).
(15) P. Tollin and D. W. Young, World List of Crystallographic Computer Programs, 3d ed, No. 41, *J. Appl. Crystallogr.*, **6**, 314 (1973).
(16) J. A. Wunderlich, *Acta Crystallogr.*, **19**, 200 (1965).
(17) W. H. Green, *J. Chem. Phys.*, **50**, 1619 (1969).
(18) G. Royer and W. J. Canady, *Arch. Biochem. Biophys.*, **124**, 530 (1968).
(19) J. J. Birktoft and D. M. Blow, *J. Mol. Biol.*, **68**, 187 (1972).
(20) R. Henderson, *J. Mol. Biol.*, **54**, 341 (1970).
(21) D. W. Ingles and J. R. Knowles, *Biochem. J.*, **104**, 369 (1967).
(22) J. H. Cross, A. Griffiths, and M. T. G. Powell, World List of Crystallographic Computer Programs, 3d ed, No. 194, 197, 198, 199, and 200, *J. Appl. Crystallogr.*, **6**, 329 (1973).
(23) J. J. Birktoft, B. W. Matthews, and D. M. Blow, *Biochem. Biophys. Res. Commun.*, **36**, 131 (1969).